

Development of Novel Benzimidazole Derivates as Potent and Selective Akt Kinase Inhibitors Using *In-silico* Approaches

Rasha Ghanem Kattoub^{1*}, Faten Sliman², Mohammad Kousara¹

¹Department of Pharmaceutical Chemistry and Quality Control, Faculty of Pharmacy, Tishreen University, Lattakia, Syria

²Department of Pharmaceutical Chemistry and Quality Control, Faculty of Pharmacy, Tartous University, Tartous, Syria

Email: *rashakattoub@tishreen.edu.sy

How to cite this paper: Kattoub, R.G., Sliman, F. and Kousara, M. (2021) Development of Novel Benzimidazole Derivates as Potent and Selective Akt Kinase Inhibitors Using *In-silico* Approaches. *International Journal of Organic Chemistry*, 11, 106-127.

<https://doi.org/10.4236/ijoc.2021.113009>

Received: August 8, 2021

Accepted: September 23, 2021

Published: September 26, 2021

Copyright © 2021 by author(s) and Scientific Research Publishing Inc. This work is licensed under the Creative Commons Attribution International License (CC BY 4.0).

<http://creativecommons.org/licenses/by/4.0/>



Open Access

Abstract

The serine/threonine Akt kinase signaling pathway plays an essential role not only in tumorigenesis but also in the potential response to anticancer therapeutic agents. Therefore, aiming to identify potent and selective Akt inhibitors, a novel series of benzimidazole derivatives were designed and docked within the crystal structure of Akt1 kinase. In order to predict their selectivity, the hit compounds were docked against the protein kinase A (PKA), which is the closely related AGC family kinase protein. Moreover, *in-silico* ADMET-related descriptors were estimated to predict the pharmacokinetic properties for the selected compounds. Among the designed molecules, four compounds were found to have the best binding affinity and good selectivity to Akt1 kinase, furthermore, those compounds had acceptable ADMET properties and were predicted to be non-mutagenic, which could account them as promising Akt1 inhibitory agents for further investigations.

Keywords

Akt, Selective ATP-competitive Inhibitors, Benzimidazole, Molecular Docking, *In-silico* ADMET

1. Introduction

Akt (Protein kinase B (PKB)) is a serine/threonine protein kinase that belongs to the AGC family group of kinases [1]. Akt family presents as three isoforms: Akt1/PKB α , Akt2/PKB β , and Akt3/PKB γ , all of which consist of three conserved structural features: an N-terminal Pleckstrin homology (PH) domain, an ATP binding central kinase domain, and a C-terminal hydrophobic motif (HM). The

three Akt members exhibit more than 80% sequence similarity in the kinase catalytic domain [2] [3].

Akt is a key mediator of the PI3K/Akt pathway that regulates a number of cellular processes including cell survival, growth, proliferation, and angiogenesis in response to many different external stimuli such as growth factors and cytokines. This wide range of effects is caused by Akt-mediated phosphorylation of numerous downstream substrates such as BAD, FOXO transcription factors, TSC2, P21^{Waf1/Cip1}, P27^{Kip1}, and eNOS [4] [5].

Studies have proved that hyperactivation of the Akt signaling cascade drives many cancers. The oncogenic alterations in many components of the PI3K/Akt pathway have been identified in approximately 40% of all human tumors [6]. Overexpression or activating mutations of upstream growth factor receptors such as EGFR and PDGFR lead to Akt activation, as do point mutations of PIK3CA, the gene encodes the catalytic p110 α subunit of PI3K, that occur in breast, colon, and endometrial cancers [5]. Additionally, inactivating mutations of the tumor suppressor phosphatidylinositol phosphatase (PTEN), a key negative regulator of this pathway, have been reported in a wide variety of cancers such as endometrial, skin, colon, ovary, and breast [7]. Finally, Akt gene itself can be amplified in several lines of cancer [8], and the transforming mutation Akt1^{E17K}, which results in constitutively active enzyme [9] [10], has been found in breast, bladder, cervix, and prostate cancers [8].

Furthermore, increasing evidence has indicated that the development of tumor cells with enhanced resistance to a wide spectrum of chemo- and radiotherapeutic agents, such as cisplatin and etoposide, is the consequence of modulated PI3K/Akt signaling system, and that treatment with targeted therapies, as EGFR inhibitors, can prompt feed-back loops involving Akt [11] [12] [13].

These findings suggest that dysregulation of Akt-dependent signaling plays a fundamental role in malignancies and drug resistance, and blocking this kinase activity could restrain the undesirable effects of this enzyme. Therefore, inhibiting Akt activity is considered a compelling approach in treating cancer and restoring sensitivity to anticancer agents.

Numerous small molecules Akt inhibitors with proven clinical benefit have been described, including the allosteric inhibitor MK-2206 (1) [14], and the ATP-competitive inhibitors GDC-0068 (Ipatasertib, 2) [15] and AZD5363 (3) [16] (Figure 1). Recently, research has expanded toward the development of selective ATP-competitive inhibitors. However, generating selective Akt inhibitors over other AGC kinases, especially the closely homologous protein kinase A (PKA), has emerged as a serious challenge due to high identity in the ATP-binding site among these enzymes, resulting in poor selectivity [17] [18]. GDC-0068, which has a PKA/Akt selectivity ratio of 620x, was able to overcome this obstruction [15]. Experimental data indicate that improving selectivity could be accomplished by exploiting key differences in the binding pockets between Akt1 and PKA. These distinctions include residues Thr211, Met281, and Ala230 in

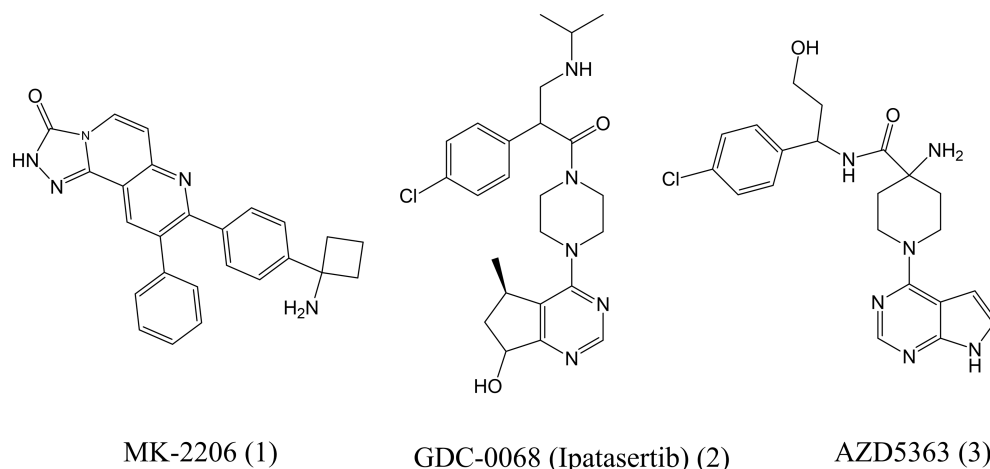


Figure 1. (1) Inactive Akt kinase allosteric inhibitor, (2 and 3) Active Akt kinase ATP-competitive inhibitors.

Akt1 to Val104, Leu173, and Val123 in PKA respectively. These differences lead to a narrower and less polar cavity in PKA, and therefore, Akt1 binding site should be more accommodating of larger substituted ligands. Thus, it could be possible to develop selective ATP-competitive Akt inhibitors [17] [18].

The drug discovery process is laborious, long-lasting, and expensive. Therefore, computer-aided drug design (CADD) strategies have become attractive approaches that can reduce the time needed to find best possible leads. The structure-based drug design (SBDD) methods, such as molecular docking, could readily improve the ability to identify, optimize, and evaluate hits in order to produce new therapeutics [19] [20]. A special attention has been dedicated to substituted benzimidazole derivatives due to their broad spectrum of biological activities such as antimicrobial [21], anthelmintic [22], antibacterial [23], anti-inflammatory [24], and anticancer [25].

Based on the abovementioned facts, herein we describe the application of SBDD techniques for the rapid discovery of new potent and selective series of benzimidazole-derived ATP-competitive inhibitors of Akt kinase. The designed compounds were evaluated for their binding ability to the active site of Akt1 kinase using molecular docking. Once identified, hits were subjected to investigate their selectivity by docking into the closely related PKA kinase. Moreover, *in-silico* ADMET-related descriptors were calculated to predict the pharmacokinetic properties of the selected compounds.

2. Materials and Methods

2.1. Database Generation

Available 3D crystal structures of Akt1 kinase were retrieved from the Protein Data Bank (PDB, <http://www.rcsb.org/>). These structures were classified on the basis of several parameters such as resolution (Å), and type of structure (Apo-enzyme or ligand-protein complex), and therefore, all collected complexes were divided based on the type of the inhibitor into two groups: the ATP-binding site inhibi-

tors (active conformer), and the allosteric site inhibitors (inactive conformer).

2.2. Receptor Preparation

The selected crystal structure was prepared through several steps that included the verifying of tautomer's, removing of resolved crystal water molecules, and correcting the chemistry of the protein by applying CHARMM forcefield. The latest procedure led to the addition of hydrogen atoms, which in turn caused steric overlap. Thus, energy minimization was carried out to solve this steric obstruction and to find the most stable and least energy conformation [26]. Once minimized, the active site was defined, and a sphere was created around the centroid of extracted ligand.

2.3. Design and Compound Library Preparation

ChemBioOffice 2008 was used to design a set of benzimidazole derivatives for the docking study. The designed ligands were then retrieved and prepared using "prepare ligands" protocol of Discovery studio 3.5.

2.4. Docking Studies

All docking procedures were performed by Discovery studio (D.S) 3.5 (Accelrys Co., Ltd., US) using the CDocker modules. CDocker is a Molecular Dynamics (MD) simulated-annealing-based algorithm which uses the CHARMM force field [27] [28]. This docking technique requires the use of both optimized and prepared protein, and all prepared compounds. Docking operations were carried out using CDocker protocol. For each compound, 10 binding poses were obtained and ranked according to their -CDocker energies (kcal/mol). The protein-ligand complexes produced after docking study were analyzed on the bases of docking scores and predicted binding mode of each docked compound [27].

For the validation of the docking procedure, native ligand was extracted and redocked using the aforementioned protocol. Docking results with RMSD (root mean standard division) less than 2.0 Å between the reference ligand in crystalized form and its 10 best reproduced conformations were considered acceptable [29].

2.5. Hits Filtration

2.5.1. Drug-Likeness Properties

The molecular properties for the candidate compounds were calculated using Discovery studio 3.5. Hits were then filtered based on the Lipinski's rule of five (RO5), which verifies whether the physiochemical properties of molecules permit them to be orally bioavailable. These drug-likeness properties include: molecular weight (MW) less than 500 Daltons, calculated LogP value less than 5, no more than 5 hydrogen bond donors (HBDs), no more than 10 hydrogen bond acceptors (HBAs), and no more than 10 rotatable bonds [30].

2.5.2. ADMET Prediction

Absorption, distribution, metabolism, excretion, and toxicity (ADMET) proper-

ties of the hit compounds were estimated using ADMET descriptors implemented in Discovery studio 3.5. The module uses six mathematical models to quantitatively predict those features by a set of rules (**Table 1**). These models predict: human intestinal absorption (HIA) after oral administration, aqueous solubility of each compound at 25°C, blood brain barrier (BBB) penetration after oral administration, cytochrome P450 2D6 (CYP2D6) enzyme inhibition, hepatotoxicity, and plasma protein binding. The intestinal absorption model, as well as the blood brain penetration model, includes 95% and 99% confidence ellipses in ADMET_AlogP98 vs. ADMET_PSA 2D plane. Selected compounds were also analyzed according to AMES mutagenicity using Discovery studio 3.5 (**Table 1**).

Table 1. Rules of ADMET-related descriptors and mutagenicity prediction used in DS 3.5.

ADMET Descriptor	Level	Description
ADMET Absorption Level (Human Intestinal Absorption (HIA))	0	Good absorption
	1	Moderate absorption
	2	Low absorption
	3	Very low absorption
ADMET Solubility Level (Aqueous Solubility Levels)	0	Extremely low
	1	No, very low, but possible
	2	Yes, low
	3	Yes, good
	4	Yes, optimal
	5	No, too soluble
ADMET Blood Brain Barrier (BBB Penetration Levels)	6	Warning: molecules with one or more unknown AlogP98 types
	0	Very High
	1	High
	2	Medium
	3	Low
	4	Undefined
ADMET Cytochrome P450 2D6 (CYP2D6) Inhibition	5	Warning: molecules with one or more unknown AlogP98 types
	0	Non-inhibitor
ADMET Hepatotoxicity	1	Inhibitor
	0	Non-hepatotoxic
ADMET PPB (Plasma Protein Binding)	1	Toxic
	0	Binding is <90%
AMES Mutagenicity	1	Binding is ≥90%
	0	Non-mutagen
	1	Mutagen

3. Results and Discussion

3.1. Akt kinase Data Analysis

The crystal structure of Akt1 in its complex with GDC-0068 (PDB code: 4EKL (DOI: <https://doi.org/10.2210/pdb4EKL/pdb>)) was found to be the most valid structure for this docking study. 4EKL has a resolution of 2.0 Å, and it is an active conformer of Akt1. The crystalized inhibitor has an IC₅₀ value of 5 nM [15].

3.2. Docking Studies

CDocker docking protocol using 4EKL was validated by redocking the native ligand which reproduced the crystalized conformer with RMSD less than 1.0 Å. The same protocol was employed to study the benzimidazole derivatives within the binding site of 4EKL. The structures and -CDocker energies (kcal/mol) of newly designed benzimidazole derivatives are represented in **Table 2**.

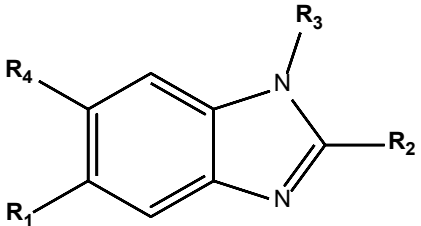
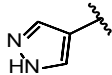
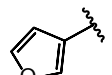
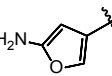
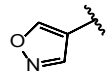
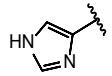
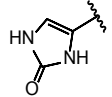
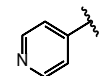
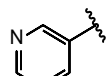
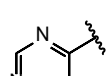
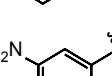
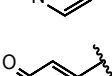
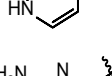
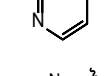
Most of the designed compounds showed good affinity towards the active site of Akt1 represented by good -CDocker energy values ranging from 22.0603 to 50.7951 kcal/mol for compounds BENZ 1 and BENZ 14 respectively (**Table 2**). Analysis of the docking results revealed that R₁ substituent occupies the adenine-binding pocket and forms a number of hydrogen bonds within the hinge region-forming residues (Glu228 and Ala230), while the protonated amine interacts with the carboxylate side chains of Glu234 and Glu278 in the acidic hole via hydrogen bonds (**Figure 2**).

In intention to investigate the effect of the alkyl linker length between the amine group and the benzimidazole ring, compounds BENZ 16 - 30 (R₂ = (CH₂)₂NH₂) were docked into the active site of Akt1 (**Table 2**). It was found that increasing the alkylamine length didn't affect the binding affinity, as most of the designed molecules maintained the same binding patterns seen in compounds BENZ 1 - 15 (R₂ = CH₂NH₂).

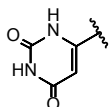
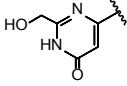
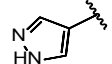
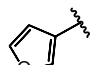
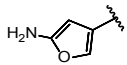
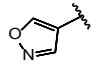
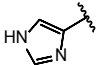
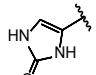
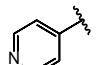
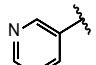
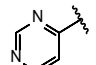
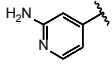
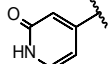
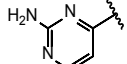
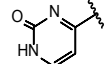
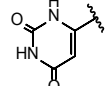
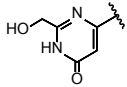
Our previous designed compounds were characterized by their ability to bind to Akt1 active site. However, they weren't able to reach the small hydrophobic pocket under the glycine-rich loop (G-loop), which is formed when Phe161 residue is displaced toward the αC helix. Therefore, benzimidazole ring was modified according to **Table 3**, where R₃ is equal to a benzyl group or a trifluoropropyl group (BENZ 31 - 54).

Docking analysis of the benzyl derivatives demonstrated higher affinity towards Akt1 active site compared to the previous compounds. Among these compounds, BENZ 34 (-CDocker energy = 55.6572 kcal/mol) had high affinity towards the active site of Akt1 enzyme. **Figure 3** demonstrates its binding mode: R₁ motif interacts via two hydrogen bonds with the backbone carbonyl of Glu228 and the main chain NH of Ala230, the primary amine group forms two hydrogen bonds within the acidic hole through residues Glu234 and Glu278, and the benzyl ring occupies the small hydrophobic pocket under the G-loop. Same interactions could be seen with BENZ 35, which showed better affinity towards the active site of Akt1 (-CDocker energy = 62.0716 kcal/mol) compared to BENZ 34.

Table 2. The structures and -CDocker energy values (kcal/mol) of the designed benzimidazole derivatives BENZ 1 - 30.

					
Co.	R ₁	R ₂	R ₃	R ₄	-CDocker energy (kcal/mol)
BENZ 1		CH ₂ NH ₂	H	H	22.0603
BENZ 2		CH ₂ NH ₂	H	H	41.1051
BENZ 3		CH ₂ NH ₂	H	H	44.7462
BENZ 4		CH ₂ NH ₂	H	H	38.4673
BENZ 5		CH ₂ NH ₂	H	H	38.0292
BENZ 6		CH ₂ NH ₂	H	H	31.5126
BENZ 7		CH ₂ NH ₂	H	H	36.1303
BENZ 8		CH ₂ NH ₂	H	H	35.6945
BENZ 9		CH ₂ NH ₂	H	H	39.1104
BENZ 10		CH ₂ NH ₂	H	H	41.8719
BENZ 11		CH ₂ NH ₂	H	H	40.6417
BENZ 12		CH ₂ NH ₂	H	H	47.7765
BENZ 13		CH ₂ NH ₂	H	H	45.0696

Continued

BENZ 14		CH ₂ NH ₂	H	H	50.7951
BENZ 15		CH ₂ NH ₂	H	H	49.5837
BENZ 16		(CH ₂) ₂ NH ₂	H	H	22.3809
BENZ 17		(CH ₂) ₂ NH ₂	H	H	41.1981
BENZ 18		(CH ₂) ₂ NH ₂	H	H	45.3790
BENZ 19		(CH ₂) ₂ NH ₂	H	H	39.5087
BENZ 20		(CH ₂) ₂ NH ₂	H	H	39.1732
BENZ 21		(CH ₂) ₂ NH ₂	H	H	32.7537
BENZ 22		(CH ₂) ₂ NH ₂	H	H	38.0449
BENZ 23		(CH ₂) ₂ NH ₂	H	H	35.6866
BENZ 24		(CH ₂) ₂ NH ₂	H	H	40.5791
BENZ 25		(CH ₂) ₂ NH ₂	H	H	43.0985
BENZ 26		(CH ₂) ₂ NH ₂	H	H	41.6491
BENZ 27		(CH ₂) ₂ NH ₂	H	H	48.4948
BENZ 28		(CH ₂) ₂ NH ₂	H	H	45.7522
BENZ 29		(CH ₂) ₂ NH ₂	H	H	52.0527
BENZ 30		(CH ₂) ₂ NH ₂	H	H	51.5375

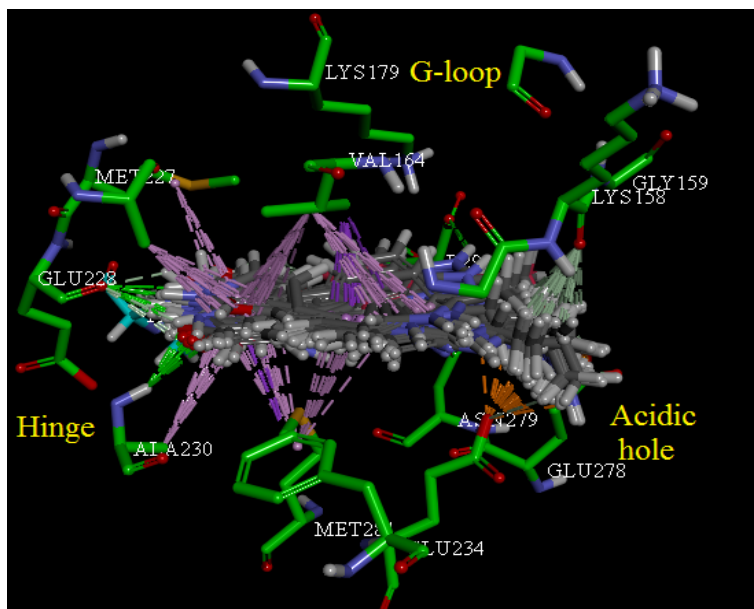
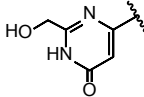
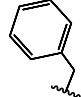
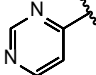
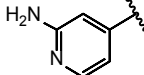
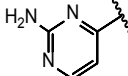
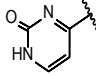
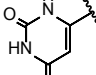
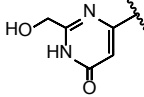
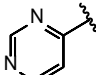
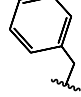
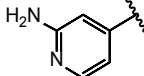
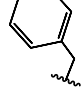
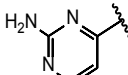
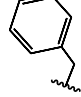
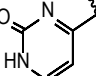
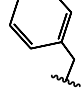
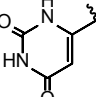
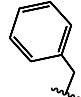
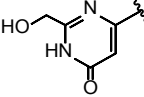
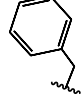
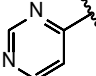


Figure 2. Superposition and binding modes of compounds BENZ 1 - 30 within the active site of Akt1 kinase.

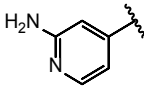
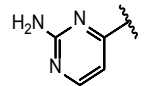
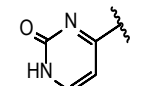
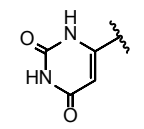
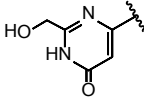
Table 3. The structures and -CDocker energy values (kcal/mol) of the designed benzimidazole derivatives BENZ 31 - 54.

					-CDocker energy (kcal/mol)
Co.	R ₁	R ₂	R ₃	R ₄	
BENZ 31		CH ₂ NH ₂		H	50.1933
BENZ 32		CH ₂ NH ₂		H	53.0033
BENZ 33		CH ₂ NH ₂		H	57.0789
BENZ 34		CH ₂ NH ₂		H	55.6572
BENZ 35		CH ₂ NH ₂		H	62.0716

Continued

BENZ 36		CH ₂ NH ₂		H	57.0868
BENZ 37		CH ₂ NH ₂	(CH ₂) ₂ CF ₃	H	44.9734
BENZ 38		CH ₂ NH ₂	(CH ₂) ₂ CF ₃	H	46.3741
BENZ 39		CH ₂ NH ₂	(CH ₂) ₂ CF ₃	H	53.3190
BENZ 40		CH ₂ NH ₂	(CH ₂) ₂ CF ₃	H	49.4578
BENZ 41		CH ₂ NH ₂	(CH ₂) ₂ CF ₃	H	56.3839
BENZ 42		CH ₂ NH ₂	(CH ₂) ₂ CF ₃	H	54.6270
BENZ 43		(CH ₂) ₂ NH ₂		H	50.1895
BENZ 44		(CH ₂) ₂ NH ₂		H	47.9918
BENZ 45		(CH ₂) ₂ NH ₂		H	52.9105
BENZ 46		(CH ₂) ₂ NH ₂		H	54.4505
BENZ 47		(CH ₂) ₂ NH ₂		H	61.8319
BENZ 48		(CH ₂) ₂ NH ₂		H	63.0024
BENZ 49		(CH ₂) ₂ NH ₂	(CH ₂) ₂ CF ₃	H	43.8223

Continued

BENZ 50		$(\text{CH}_2)_2\text{NH}_2$	$(\text{CH}_2)_2\text{CF}_3$	H	46.8861
BENZ 51		$(\text{CH}_2)_2\text{NH}_2$	$(\text{CH}_2)_2\text{CF}_3$	H	50.5165
BENZ 52		$(\text{CH}_2)_2\text{NH}_2$	$(\text{CH}_2)_2\text{CF}_3$	H	47.5281
BENZ 53		$(\text{CH}_2)_2\text{NH}_2$	$(\text{CH}_2)_2\text{CF}_3$	H	56.0871
BENZ 54		$(\text{CH}_2)_2\text{NH}_2$	$(\text{CH}_2)_2\text{CF}_3$	H	55.0972

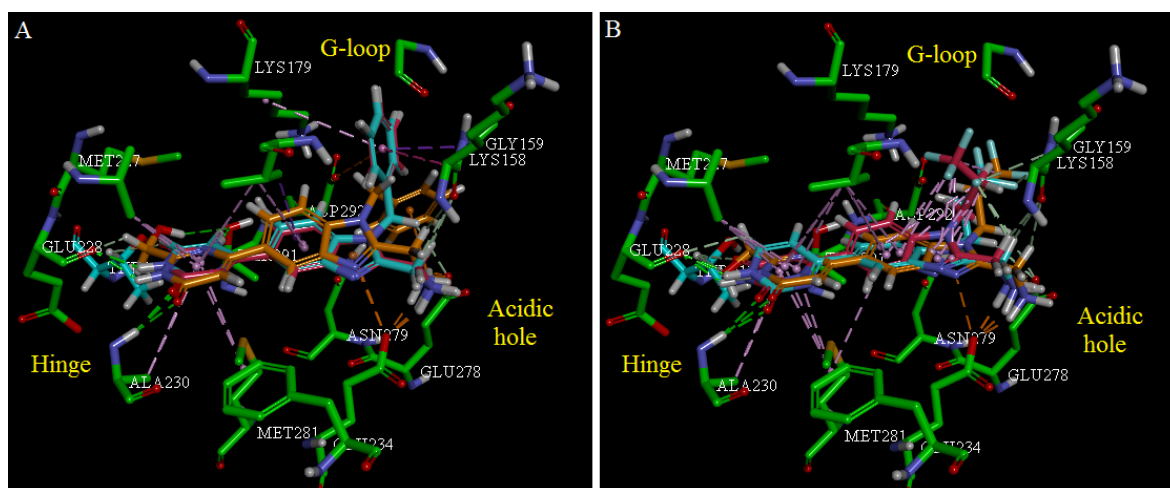


Figure 3. Superposition and binding mode of (A) compounds BENZ 34 - 35 and 36 (shown in cyan, magenta, and brown respectively), (B) their fluorinated counterparts BENZ 40 - 41 and 42 (shown in cyan, magenta, and brown respectively) within the active site of Akt1 kinase.

The pyrimidinedione ring interacts with the kinase hinge through its 1-NH and carbonyl group, and residues Glu228 and Ala230 respectively. On the other hand, 3-NH group forms a hydrogen bond with Thr291, while the other carbonyl group is positioned near the hydrophilic side chain of the gatekeeper residue Thr211. Replacing the carbonyl group in compound BENZ 35 with a hydroxymethyl group led to compound BENZ 36, which exhibited a decrease in its affinity (Table 3). This result seems to be because of this structural alteration that caused the benzyl group to be located away from the pocket under G-loop, while this group is optimally positioned to occupy this pocket in compound BENZ 35 as shown in Figure 3.

Trifluoropropyl derivatives (BENZ 37 - 42) showed a slight decrease in their

affinity compared to their benzyl analogs (BENZ 31 - 36). According to the *in-silico* docking results, it was observed that the fluorinated substituent is located within the G-loop hydrophobic pocket, but it can't reach this pocket deep enough, as shown with compounds BENZ 40, 41 and 42 (Figure 3).

Similar to the previous study, we replaced R₂ substituent with an ethylamine group to afford compounds BENZ 43 - 54 in order to detect the effect of R₂ substituent length. In both the benzyl and trifluoropropyl derivatives, this increase in alkyl length was not associated with an increase in binding affinity as most of the designed molecules maintained the same interactions as indicated by the superposition of compound BENZ 35 and its ethylamine derivative BENZ 47, and compound BENZ 41 and its derivative BENZ 53 shown in Figure 4.

Finally, we fixed R₃ as a benzyl group, then turned our attention to study the effect of amine substitution in conjunction with the introduction of a methyl group at benzimidazole C6 in order to find more effective compounds that are able to exploit the binding site of Akt1 (Table 4).

Most of the designed molecules showed a similar binding mode whereby the methyl group is placed within a small hydrophobic pocket formed by the side chains of Val164 and Lys179. The substituted amine maintained its ability to form hydrogen bonds with the carboxylate side chain of acidic hole residues Glu234 and Glu278, while the aliphatic and cyclic substitutions of the amine located in the solvent-exposed region without significantly affecting the binding affinity of these compounds as exemplified by compounds BENZ 56 and BENZ 57 shown in Figure 5. These compounds fit well inside the binding site creating two hydrogen bonds with Glu228 and Ala230 amino acids, whilst the benzyl group occupies the small hydrophobic pocket under G-loop.

Compounds BENZ 62 and BENZ 63, which bears a hydroxymethyl group substituted on R₁ motif, showed higher-CDocker energy of 60.0004 and 61.1954

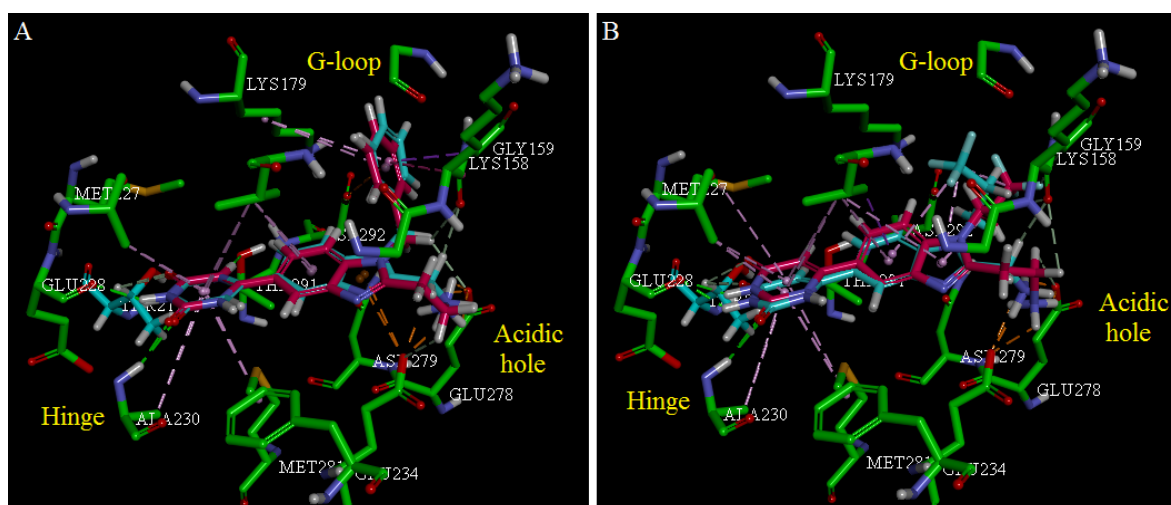


Figure 4. Superposition and binding mode of (A) compounds BENZ 35 and BENZ 47 (shown in cyan and magenta respectively), (B) compounds BENZ 41 and BENZ 53 (shown in cyan and magenta respectively) within the active site of Akt1 kinase.

Table 4. The structures and -CDocker energy values (kcal/mol) of the designed benzimidazole derivatives BENZ 55 - 66.

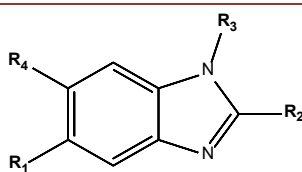
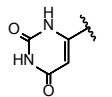
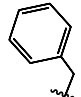
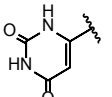
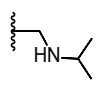
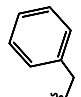
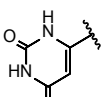
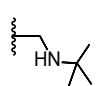
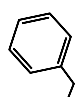
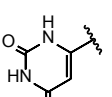
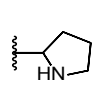
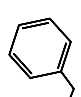
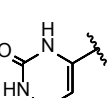
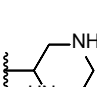
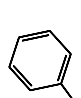
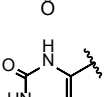
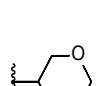
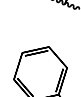
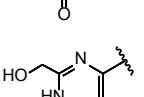
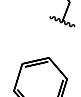
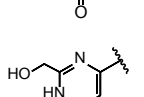
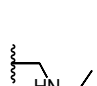
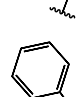
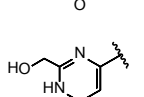
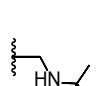
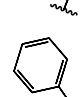
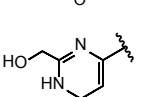
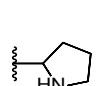
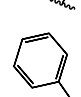
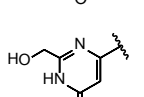
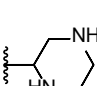
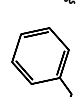
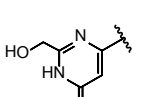
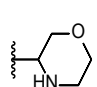
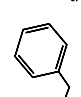
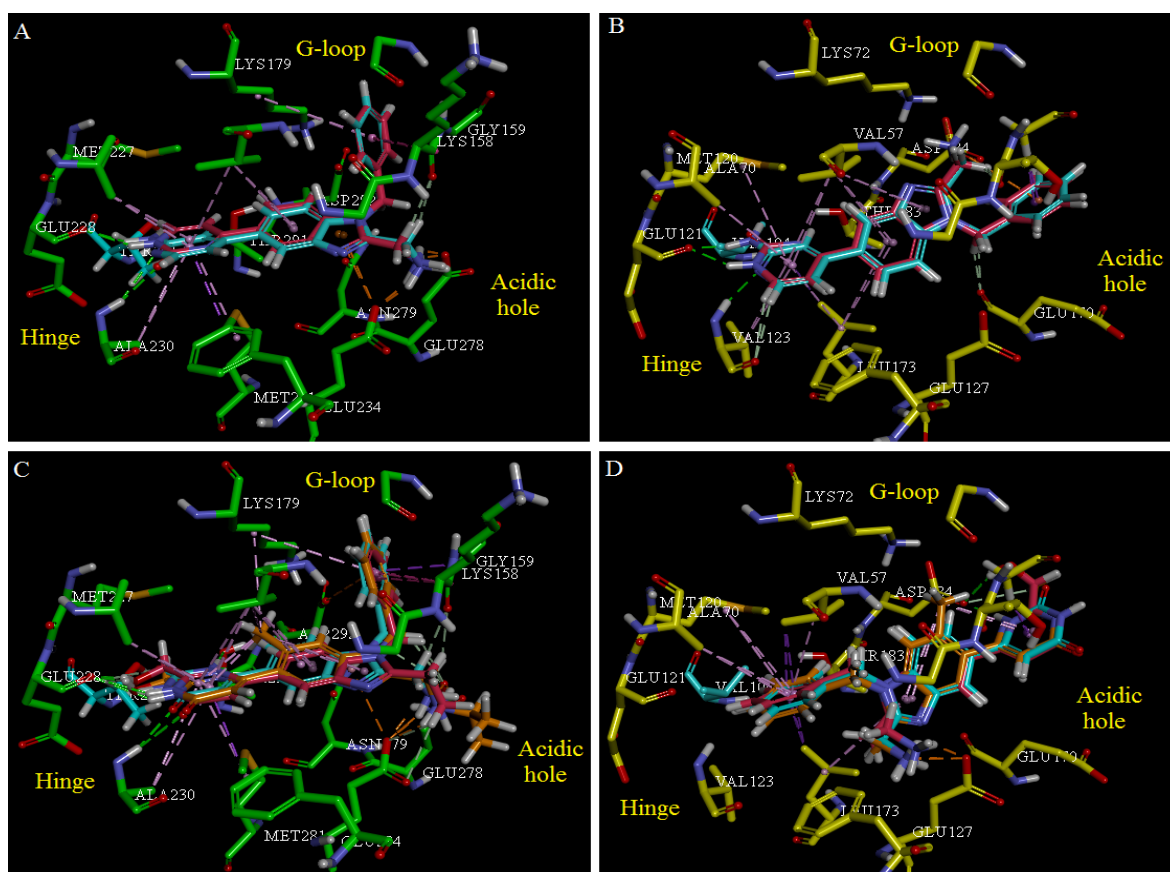
					-CDocker energy (kcal/mol)
Co.	R ₁	R ₂	R ₃	R ₄	
BENZ 55		CH ₂ NH ₂		CH ₃	61.2076
BENZ 56				CH ₃	62.0965
BENZ 57				CH ₃	60.2102
BENZ 58				CH ₃	42.4818
BENZ 59				CH ₃	57.0188
BENZ 60				CH ₃	59.3709
BENZ 61		CH ₂ NH ₂		CH ₃	61.1409
BENZ 62				CH ₃	60.0004
BENZ 63				CH ₃	61.1954
BENZ 64				CH ₃	41.4988
BENZ 65				CH ₃	52.3016
BENZ 66				CH ₃	54.9118

Table 5. -CDocker energy values (kcal/mole) of designed benzimidazole hits resulted from docking within the active site of PKA.

Co.	-CDocker energy (kcal/mol)
BENZ 32	27.2281
BENZ 34	30.6591
BENZ 35	36.9788
BENZ 48	31.2675
BENZ 56	7.09464
BENZ 57	-39.4743
BENZ 61	34.1176
BENZ 62	-28.8812
BENZ 63	-101.662
BENZ 66	-69.9333

**Figure 6.** Comparison of the binding mode of compounds BENZ 32 - 34 (shown in cyan and magenta respectively) within the active site of (A) Akt1 kinase, (B) PKA, and compounds BENZ 35 - 48 - 61 (shown in cyan, magenta, and brown respectively) within the active site of (C) Akt1 kinase, (D) PKA.

Though compounds BENZ 35 - 48 - 61 showed a good -CDocker energy (Table 5), docking results analysis revealed that these compounds had a different binding mode within the ATP-binding pocket of both Akt1 and PKA, as the

benzyl group occupied the adenine-binding pocket of the later with no bonds identified with the hinge-forming residues, whereas R₁ is placed towards outside ATP-binding pocket. It is possible to construe these results to R₁ carbonyl group (compound BENZ 35) and hydroxymethyl group (compounds BENZ 48 and BENZ 61), which is positioned near the hydrophilic side chain of the gatekeeper residue Thr211. This binding pattern is expected to be undesirable in the case of the ATP-binding site of PKA, where the hydrophobic Val104 is the corresponding residue (**Figure 6**).

This study has demonstrated that compounds BENZ 56-57-62-63-66 has high selectivity against the active site of PKA (**Table 5**). These results indicate the importance of the substitution of the amine with bulkier groups and the introduction of a methyl group on benzimidazole C6, as these modifications didn't compromise the binding affinity of the designed compounds towards Akt1 active site, but they were not tolerated by PKA.

It should be noted that the most selective compound BENZ 63 (-CDocker energy (Akt1) = 61.1954, (PKA) = -101.662 kcal/mol) have a hydroxymethyl group substituted on the hinge-binding motif (R₁) instead of a carbonyl group in compound BENZ 57, and differs from compound BENZ 61 by the presence of a *t*-Bu group substituted on the amine. This result can be justified by the dual effect of the hydroxymethyl group that can reach deep and locate in the vicinity of the hydrophilic side chain of Akt1 gatekeeper residue Thr211, and the significance of the substitution of the amine described above. **Figure 7** displays the difference in the binding mode of compound BENZ 63 within the ATP-binding site of Akt1 and PKA.

3.4. Hits Filtration

3.4.1. Drug-Likeness Properties

Much of the drug oral bioavailability is influenced by its solubility and ability to pass the intestinal wall, which in turn relates to the physicochemical properties of

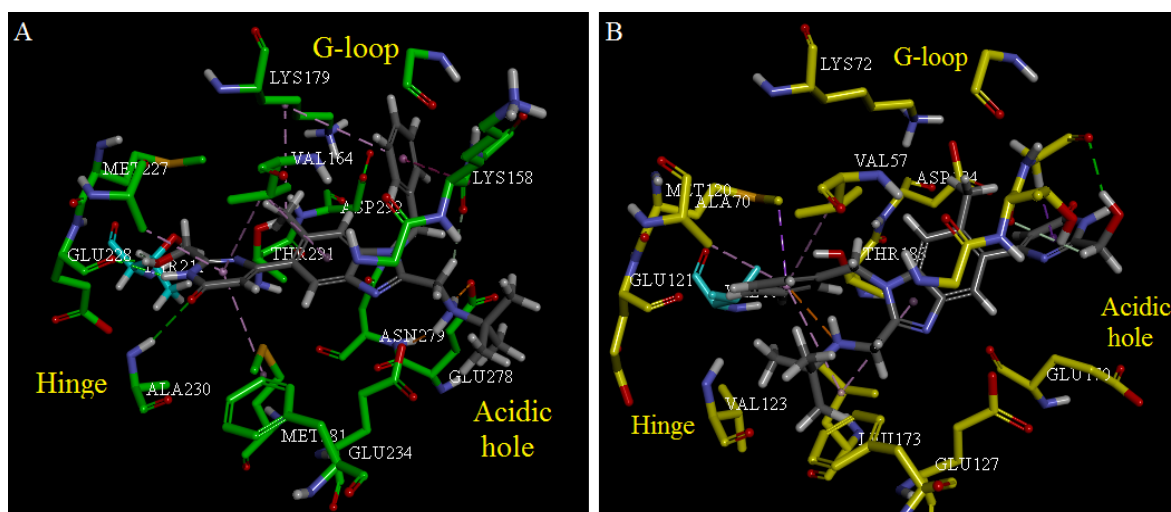


Figure 7. Comparison of the binding mode of compound BENZ 63 within the active site of (A) Akt1 kinase, (B) PKA.

the drug molecule such as water solubility, LogP, hydrogen bonding characteristics, flexibility, etc. [32]. Therefore, the molecular properties of the hits were calculated, then these molecules were filtered based on Lipinski's rule of five (RO5).

All of the selected compounds were found to be within the accepted range of RO5 parameters, and thus these compounds are expected to have good bioavailability after oral administration (Table 6).

3.4.2. *In-silico* ADMET Study

ADMET properties play a significant role during the drug development process, as they are found to be responsible for the failure of 60% of drug molecules [32]. These properties mostly affect the drug bioavailability, cell permeation, and metabolism which are important descriptor in drug discovery research. Table 7 summarizes the ADMET properties of the selected compounds.

Polar surface area (PSA) was shown to have an inverse relationship with human intestinal absorption and thus cellular permeability [33]. Although the relationship between PSA and cellular permeability has been demonstrated, the models usually do not take into account the influence of other descriptors. The lipophilic properties of the molecule can be assessed by calculating the octanol/water partition coefficient (LogP). Though LogP is generally used in estimating the lipophilic properties of the compound, the fact that LogP is a ratio raises concern about its use for estimating hydrophilic and lipophilic properties [34]. Therefore, hydrogen bonding characteristics obtained through PSA can be taken along with LogP values [35]. Thus, AlogP98 and PSA_2D model with a binary plot comprising 95% and 99% confidence ellipses were used to accurately predict the cellular permeability of the selected compounds [35].

Table 6. Molecular properties and Lipinski's rule of five parameters of benzimidazole hits.

Co.	ALogP	MW	Num. HBDs	Num. HBAs	Num. Rot. Bonds	Num. Rings	Num. Ar. Rings	MFPSA
BENZ 32	1.589	330.406	2	3	4	4	4	0.245
BENZ 34	1.044	332.379	2	3	4	4	3	0.259
BENZ 35	0.336	348.379	3	3	4	4	3	0.303
BENZ 48	0.176	376.432	3	4	6	4	3	0.280
BENZ 56	1.754	404.485	3	3	6	4	3	0.220
BENZ 57	1.959	418.511	3	3	6	4	3	0.205
BENZ 61	0.414	376.432	3	4	5	4	3	0.277
BENZ 62	1.347	418.511	3	4	7	4	3	0.216
BENZ 63	1.552	432.538	3	4	7	4	3	0.203
BENZ 66	0.443	432.495	3	5	5	5	3	0.242

MW: Molecular Weight, MFPSA: Molecular Fractional Polar Surface Area.

According to the model, in order to have optimal cellular permeability the compound should meet the following criteria: $PSA_{2D} < 140 \text{ \AA}^2$ and $AlogP_{98} < 5$ [35]. All hits showed $PSA_{2D} < 140 \text{ \AA}^2$, as the upper limit reached 111.113 \AA^2 (BENZ 48 and BENZ 61), while the lower limit was 76.831 \AA^2 (BENZ 56 and BENZ 57), and all compounds had $AlogP_{98}$ values < 5 .

All candidates fell within the 99% confidence ellipse regarding absorption (Figure 8), and therefore these compounds are expected to have good human intestinal absorption. All molecules showed poor ability to cross the blood-brain

Table 7. *In-silico* ADMET and mutagenic properties of benzimidazole hits.

Co.	<i>In-silico</i> ADMET and Mutagenic properties								
	Absorption	BBB penetration	Solubility	CYP26D inhibition	Hepatotoxicity	PPB	AMES mutagenicity	AlogP98	PSA-2D
BENZ 32	0	3	3	0	0	1	1	1.589	86.664
BENZ 34	0	3	3	0	0	1	0	1.044	90.297
BENZ 35	0	3	3	0	1	0	0	0.530	109.085
BENZ 56	0	3	3	0	1	0	0	1.949	76.831
BENZ 48	0	4	3	0	0	1	0	0.176	111.113
BENZ 57	0	3	2	0	1	1	0	2.154	76.831
BENZ 61	0	3	3	0	1	1	0	0.414	111.113
BENZ 62	0	3	3	0	0	1	0	1.347	78.859
BENZ 63	0	3	3	0	0	1	0	1.552	78.859
BENZ 66	0	3	3	0	0	0	0	0.443	87.789

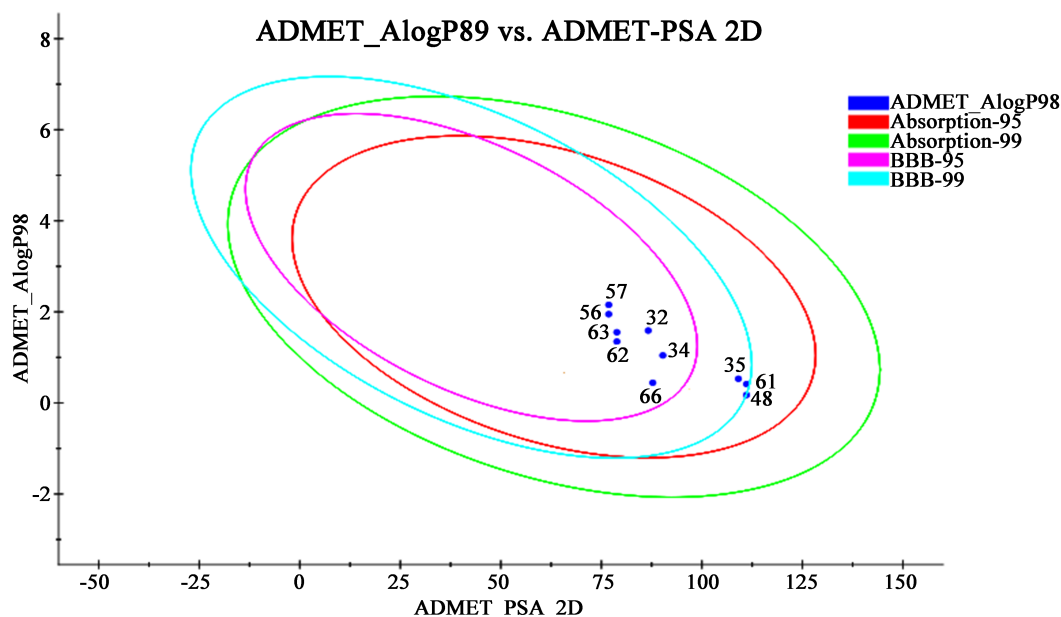


Figure 8. Calculated ADMET_ALogP98 vs. ADMET_PSA 2D plot for candidate compounds showing 95% and 99% confidence ellipses corresponding to human intestinal absorption (HIA) and blood brain barrier (BBB) penetration models.

barrier (levels 3 and 4 as stated in **Table 1**). Aqueous solubility plays a critical role in drug oral bioavailability. According to the model, all of the designed compounds, except for BENZ 57 (Level 2), have been shown to have good aqueous solubility (**Table 7**). CYP2D6 isoenzyme is involved in the metabolism of a large number of drugs, and its inhibition by a drug can lead to serious drug-drug interactions [36]. **Table 7** indicates that all of our designed compounds don't possess CYP2D6 inhibitory activity. Drug distribution from plasma to target tissues can be affected by several factors, and binding to plasma proteins is considered the most important one [37]. Compounds BENZ 35 - 56 - 66 showed binding < 90%, and therefore they are unlikely to be strongly bound to serum carrier proteins, while the remaining compounds showed binding \geq 90% (**Table 7**). Some of our selected compounds showed potential hepatotoxicity (BENZ 35-56-57-61), while compounds BENZ 32 exhibited potential mutagenicity (**Table 7**).

4. Conclusion

This study focused on designing, molecular docking, and *in-silico* ADMET evaluation of a new set of benzimidazole derivatives as potential selective Akt inhibitors. Molecular docking is used to identify potential inhibitor of Akt kinase by determining their binding energies. The most promising hits were then docked into the binding site of PKA kinase to predict their selectivity against other AGC family kinases. Among our designed molecules, eight compounds showed the best binding affinity and selectivity to Akt1 kinase. Moreover, *in-silico* ADMET and mutagenic properties prediction were carried out on these compounds. As a result, four Compounds (BENZ 48, BENZ 62, BENZ 63 and BENZ 66) had acceptable ADMET properties (with compound BENZ 66 passing the whole ADMET tests), and were predicted to be non-mutagenic. The aforementioned top hits obtained from this study can be further synthesized and evaluated by *in-vitro* and *in-vivo* biological tests.

Conflicts of Interest

The authors declare no conflicts of interest regarding the publication of this paper.

References

- [1] Arencibia, J.M., Pastor-Flores, D., Bauer, A.F., Schulze, J.O. and Biondi, R.M. (2013) AGC Protein Kinases: From Structural Mechanism of Regulation to Allosteric Drug Development for the Treatment of Human Diseases. *Biochim Biophys Acta*, **1834**, 1302-1321. <https://doi.org/10.1016/j.bbapap.2013.03.010>
- [2] Nitulescu, G.M., Margina, D., Juzenas, P., Peng, Q., Oлару, O.T., Saloustros, E., *et al.* (2016) Akt Inhibitors in Cancer Treatment: The Long Journey from Drug Discovery to Clinical Use (Review). *International Journal of Oncology*, **48**, 869-885. <https://doi.org/10.3892/ijo.2015.3306>
- [3] Osaki, M., Oshimura, M. and Ito, H. (2004) PI3K-AKT Pathway: Its Functions and

- Alterations in Human Cancer. *Apoptosis*, **9**, 667-676.
<https://doi.org/10.1023/B:APPT.0000045801.15585.dd>
- [4] Manning, B.D. and Cantley, L.C. (2007) Akt/PKB Signaling: Navigating Downstream. *Cell*, **129**, 1261-1274. <https://doi.org/10.1016/j.cell.2007.06.009>
- [5] Vasudevan, K.M. and Garraway, L.A. (2010) AKT Signaling in Physiology and Disease. In: Rommel, C., Vanhaesebroeck, B. and Vogt, P., Eds., *Phosphoinositide 3-Kinase in Health and Disease*, Vol. 347, Springer, Berlin, Heidelberg, 105-133.
https://doi.org/10.1007/82_2010_66
- [6] Millis, S.Z., Ikeda, S., Reddy, S., Gatalica, Z. and Kurzrock, R. (2016) Landscape of Phosphatidylinositol-3-Kinase Pathway Alterations across 19784 Diverse Solid Tumors. *JAMA Oncology*, **2**, 1565-1573. <https://doi.org/10.1001/jamaoncol.2016.0891>
- [7] Mundi, P.S., Sachdev, J., McCourt, C. and Kalinsky, K. (2016) AKT in Cancer: New Molecular Insights and Advances in Drug Development. *British Journal of Clinical Pharmacology*, **82**, 943-956. <https://doi.org/10.1111/bcp.13021>
- [8] Brown, J.S. and Banerji, U. (2017) Maximising the Potential of Akt Inhibitors as Anti-Cancer Treatments. *Pharmacology & Therapeutics*, **172**, 101-115.
<https://doi.org/10.1016/j.pharmthera.2016.12.001>
- [9] Carpten, J.D., Faber, A.L., Horn, C., Donoho, G.P., Briggs, S.L., Robbins, C.M., *et al.* (2007) A Transforming Mutation in the Pleckstrin Homology Domain of Akt1 in Cancer. *Nature*, **448**, 439-444. <https://doi.org/10.1038/nature05933>
- [10] Landgraf, K.E., Pilling, C. and Falke, J.J. (2008) Molecular Mechanism of an Oncogenic Mutation That Alters Membrane Targeting: Glu17Lys Modifies the PIP Lipid Specificity of the AKT1 Ph Domain. *Biochemistry*, **47**, 12260-12269.
<https://doi.org/10.1021/bi801683k>
- [11] Huang, W.C. and Hung, M.C. (2009) Induction of Akt Activity by Chemotherapy Confers Acquired Resistance. *Journal of the Formosan Medical Association*, **108**, 180-194. [https://doi.org/10.1016/S0929-6646\(09\)60051-6](https://doi.org/10.1016/S0929-6646(09)60051-6)
- [12] Cassinelli, G., Zuco, V., Gatti, L., Lanzi, C., Zaffaroni, N., Colombo, D., *et al.* (2013) Targeting the Akt Kinase to Modulate Survival, Invasiveness and Drug Resistance of Cancer Cells. *Current Medicinal Chemistry*, **20**, 1923-1945.
<https://doi.org/10.2174/09298673113209990106>
- [13] Iida, M., Harari, P.M., Wheeler, D.L. and Toulany, M. (2020) Targeting Akt/PKB to Improve Treatment Outcomes for Solid Tumors. *Mutation Research/Fundamental and Molecular Mechanisms of Mutagenesis*, **819-820**, Article ID: 111690.
<https://doi.org/10.1016/j.mrfmmm.2020.111690>
- [14] Hirai, H., Sootome, H., Nakatsuru, Y., Miyama, K., Taguchi, S., Tsujioka, K., *et al.* (2010) Mk-2206, an Allosteric AKT Inhibitor, Enhances Antitumor Efficacy by Standard Chemotherapeutic Agents or Molecular Targeted Drugs *in Vitro* and *in Vivo*. *Molecular Cancer Therapeutics*, **9**, 1956-1967.
<https://doi.org/10.1158/1535-7163.MCT-09-1012>
- [15] Blake, J.F., Xu, R., Bencsik, J.R., Xiao, D., Kallan, N.C., Schlachter, S., *et al.* (2012) Discovery and Preclinical Pharmacology of a Selective ATP-Competitive Akt Inhibitor (GDC-0068) for the Treatment of Human Tumors. *Journal of Medicinal Chemistry*, **55**, 8110-8127. <https://doi.org/10.1021/jm301024w>
- [16] Addie, M., Ballard, P., Buttar, D., Crafter, C., Currie, G., Davies, B.R., *et al.* (2013) Discovery of 4-Amino-*N*-[(1*S*)-1-(4-Chlorophenyl)-3-Hydroxypropyl]-1-(7*H*-Pyrrolo[2,3-*d*]Pyrimidin-4-*Yl*)Piperidine-4-Carboxamide (AZD5363), an Orally Bioavailable, Potent Inhibitor of Akt Kinases. *Journal of Medicinal Chemistry*, **56**, 2059-2073.
<https://doi.org/10.1021/jm301762v>

- [17] Bencsik, J.R., Xiao, D., Blake, J.F., Kallan, N.C., Mitchell, I.S., Spencer, K.L., *et al.* (2010) Discovery of Dihydrothieno- and Dihydrofuroypyrimidines as Potent Pan Akt Inhibitors. *Bioorganic & Medicinal Chemistry Letters*, **20**, 7037-7041. <https://doi.org/10.1016/j.bmcl.2010.09.112>
- [18] Wu, K., Pang, J., Song, D., Zhu, Y., Wu, C., Shao, T., *et al.* (2015) Selectivity Mechanism of ATP-Competitive Inhibitors for PKB and PKA. *Chemical Biology & Drug Design*, **86**, 9-18. <https://doi.org/10.1111/cbdd.12472>
- [19] Leelananda, S.P. and Lindert, S. (2016) Computational Methods in Drug Discovery. *Beilstein Journal of Organic Chemistry*, **12**, 2694-2718. <https://doi.org/10.3762/bjoc.12.267>
- [20] Sliwoski, G., Kothiwale, S., Meiler, J. and Lowe, E.W. (2014) Computational Methods in Drug Discovery. *Pharmacological Reviews*, **66**, 334-395. <https://doi.org/10.1124/pr.112.007336>
- [21] Ansari, K.F. and Lal, C. (2009) Synthesis, Physicochemical Properties and Antimicrobial Activity of Some New Benzimidazole Derivatives. *European Journal of Medicinal Chemistry*, **44**, 4028-4033. <https://doi.org/10.1016/j.ejmech.2009.04.037>
- [22] Sreena, K., Ratheesh, R., Rachana, M., Poornima, M. and Shyni, C. (2009) Synthesis and Anthelmintic Activity of Benzimidazole Derivatives. *Hygeia*, **1**, 21-22.
- [23] Srivastava, R., Gupta, S.K., Naaz, F., Singh, A., Singh, V.K., Verma, R., *et al.* (2018) Synthesis, Antibacterial Activity, Synergistic Effect, Cytotoxicity, Docking and Molecular Dynamics of Benzimidazole Analogues. *Computational Biology and Chemistry*, **76**, 1-16. <https://doi.org/10.1016/j.compbiolchem.2018.05.021>
- [24] Rathore, A., Sudhakar, R., Ahsan, M.J., Ali, A., Subbarao, N., Jadav, S.S., *et al.* (2017) *In Vivo* Anti-Inflammatory Activity and Docking Study of Newly Synthesized Benzimidazole Derivatives Bearing Oxadiazole and Morpholine Rings. *Bioorganic Chemistry*, **70**, 107-117. <https://doi.org/10.1016/j.bioorg.2016.11.014>
- [25] Cheong, J.E., Zaffagni, M., Chung, I., Xu, Y., Wang, Y., Jernigan, F.E., *et al.* (2018) Synthesis and Anticancer Activity of Novel Water Soluble Benzimidazole Carbamates. *European Journal of Medicinal Chemistry*, **144**, 372-385. <https://doi.org/10.1016/j.ejmech.2017.11.037>
- [26] Brooks, B.R., Bruccoleri, R.E., Olafson, B.D., States, D.J., Swaminathan, S.A. and Karplus, M. (1983) CHARMM: A Program for Macromolecular Energy, Minimization, and Dynamics Calculations. *Journal of Computational Chemistry*, **4**, 187-217. <https://doi.org/10.1002/jcc.540040211>
- [27] Kalathiya, U., Padariya, M. and Baginski, M. (2014) Molecular Modeling and Evaluation of Novel Dibenzopyrrole Derivatives as Telomerase Inhibitors and Potential Drug for Cancer Therapy. *IEEE/ACM Transactions on Computational Biology and Bioinformatics*, **11**, 1196-1207. <https://doi.org/10.1109/TCBB.2014.2326860>
- [28] Wang, Q., He, J., Wu, D., Wang, J., Yan, J. and Li, H. (2015) Interaction of *A*-Cyperone with Human Serum Albumin: Determination of the Binding Site by Using Discovery Studio and Via Spectroscopic Methods. *Journal of Luminescence*, **164**, 81-85. <https://doi.org/10.1016/j.jlumin.2015.03.025>
- [29] Wang, S., Jiang, J.-H., Li, R.-Y. and Deng, P. (2020) Docking-Based Virtual Screening of T β r1 Inhibitors: Evaluation of Pose Prediction and Scoring Functions. *BMC Chemistry*, **14**, Article No. 52. <https://doi.org/10.1186/s13065-020-00704-3>
- [30] Lipinski, C.A., Lombardo, F., Dominy, B.W. and Feeney, P.J. (2001) Experimental and Computational Approaches to Estimate Solubility and Permeability in Drug Discovery and Development Settings. *Advanced Drug Delivery Reviews*, **46**, 3-26. [https://doi.org/10.1016/S0169-409X\(00\)00129-0](https://doi.org/10.1016/S0169-409X(00)00129-0)

- [31] Müller, J., Kirschner, R.A., Geyer, A. and Klebe, G. (2019) Conceptual Design of Self-Assembling Bisubstrate-Like Inhibitors of Protein Kinase a Resulting in a Boronic Acid Glutamate Linkage. *ACS Omega*, **4**, 775-784. <https://doi.org/10.1021/acsomega.8b02364>
- [32] Mandlik, V., Bejugam, P.R. and Singh, S. (2016) Application of Artificial Neural Networks in Modern Drug Discovery. In: Puri, M., Pathak, Y., Kumar Sutariya, V., Tipparaju, S. and Moreno, W., Eds., *Artificial Neural Network for Drug Design, Delivery and Disposition*, Academic Press, Cambridge, 123-139. <https://doi.org/10.1016/B978-0-12-801559-9.00006-5>
- [33] Palm, K., Stenberg, P., Luthman, K. and Artursson, P. (1997) Polar Molecular Surface Properties Predict the Intestinal Absorption of Drugs in Humans. *Pharmaceutical Research*, **14**, 568-571. <https://doi.org/10.1023/A:1012188625088>
- [34] Leo, A., Hansch, C. and Elkins, D. (1971) Partition Coefficients and Their Uses. *Chemical Reviews*, **71**, 525-616. <https://doi.org/10.1021/cr60274a001>
- [35] Egan, W.J., Merz, K.M., and Baldwin, J.J. (2000) Prediction of Drug Absorption Using Multivariate Statistics. *Journal of Medicinal Chemistry*, **43**, 3867-3877. <https://doi.org/10.1021/jm000292e>
- [36] Storelli, F., Matthey, A., Lenglet, S., Thomas, A., Desmeules, J. and Daali, Y. (2018) Impact of *CYP2D6* Functional Allelic Variations on Phenoconversion and Drug-Drug Interactions. *Clinical Pharmacology & Therapeutics*, **104**, 148-157. <https://doi.org/10.1002/cpt.889>
- [37] Wanat, K. (2020) Biological Barriers, and the Influence of Protein Binding on the Passage of Drugs across Them. *Molecular Biology Reports*, **47**, 3221-3231. <https://doi.org/10.1007/s11033-020-05361-2>